Effects of elastic ball and coating on pure squeeze EHL motion for constant load with couple stresses using FDM method

Li-Ming Chu[1], *Yuh-Ping* Chang[2,*], and *Jaw-Ren* Lin[3]

[1]Department of Applied Science/Interdisciplinary Program of Green and Information Technology, National Taitung University, Taitung City 95092, Taiwan, R.O.C.
[2]Department of Mechanical Engineering, Kun Shan University, Tainan City 71070, Taiwan, R.O.C.
[3]Department of Mechanical Engineering, Nanya Institute of Technology, Taoyuan City 32091, Taiwan, R.O.C.

Abstract. In this paper, an elastic sphere approaching a lubricated elastic coating surface with couple stress lubricant is explored under constant load condition. The finite difference method (FDM), Gaussian elimination, and Gauss-Seidel iteration method are used to solve the transient modified Reynolds equation with its boundary condition, the elasticity deformation equations of ball and coating layer, load balance equation, and lubricant rheology equations simultaneously. The transient pressure profiles, film shapes, and elastic deformation during the pure squeeze process under various operating conditions in the elastohydrodynamic lubrication (EHL) regime are discussed.

1 Introduction

Many mechanical elements with contact pairs such as gear teeth, cams /followers, piston ring/cylinder, rolling element bearings, and the stretching process of metal sheets occurred elastic dimple at the center of the contact region due to the squeeze effects, reveal the elastohydrodynamic lubrication (EHL) problem. Surface coatings have long been used in industrial technologies, as they can reduce friction and wear, and thus improve the service life of mechanical components. Therefore, the characteristics of an isotropic elastic coating/elastic substrate with non-Newtonian lubricants in the EHL region need to be further investigated.

To solve the formation of the dimple in pure squeeze motion problems, many numerical solutions have been proposed, including those by Yang and Wen [1], and Chang [2]. In these studies, the ball dropping case is often used since it includes all the effects of pure squeeze motion which are of interest. Dowson and Wang [3] and Larsson and Högund [4] analyzed the bouncing of an elastic sphere on an oily plate. These analyses were restricted to normal motion in the first instance in order to develop the numerical technique and to relate the overall findings to the results presented by Safa and Gohar [5].

To solve the coupled hydrodynamic equation and elasticity equation of an EHL problem, the elasticity modulus and thickness of the coating are important parameters. Many studies have treated the coating and contact surfaces as linear elastic isotropic materials. Elsharkawy and Hamrock [6] used the deformation model developed by Johnson [7] to explore the Newtonian EHL of an elastic coated surface on a rigid cylinder and rigid substrate. Jaffar [8] derived a new set of explicit expressions for the contact pressure, total load, and penetration depth for the frictionless indentation problem of a spherical punch and a bounded thick elastic layer. Liu et al. [9] developed a coating EHL model for point contacts by combining the DC-FFT algorithm for the elastic deformation of a coated surface with the unified mixed EHL model. Habchi [10] developed a full system approach to analyze a thermal EHL problem in coated circular contacts with an equivalent cube under steady state condition. Chu et al. [11] analysed a rigid sphere approaching a lubricated flat surface with a layer of elastic coating on the elastic substrate is explored under constant load conditions. But, study of EHL in pure squeeze motion on coated surface with couple stress lubricant is lacking.

In this paper, pure squeeze EHL motion of circular contacts with coating is explored under constant load condition. The finite difference method and the Gauss-Seidel iteration method are used to solve the transient modified Reynolds equation, the elasticity deformation equation, load balance equation, and lubricant rheology equations simultaneously. The transient pressure profiles and film shapes during the pure squeeze process under various operating conditions in the EHL regime are discussed.

2 Theoretical analysis

2.1 Reynolds equation

* Corresponding author: ypc0318@mail.ksu.edu.tw

According to the Stokes micro continuum theory [12], the field equations of a coupled stress fluid in the absence of body forces and body couples are

$$\nabla \cdot \mathbf{V} = 0 \tag{1}$$

$$\rho D\mathbf{V}/Dt = -\nabla p + (\mu - \eta\nabla^2)\nabla^2\mathbf{V} \tag{2}$$

where $\mathbf{V}$ is the velocity vector, ρ is the density, p is the pressure, μ is the classical viscosity coefficient, and η is a new material constant with the dimension of momentum responsible for the couple stress fluid property. Since the ratio η/μ has the dimensions of length squared, the dimension of $l = (\eta/\mu)^{1/2}$ characterizes the material length of couple stress fluids, and l is assumed to be a material constant in the present analysis.

For EHL problems, two spheres approach each other can be expressed as an equivalent sphere approaching a plane. In Figure 1, an elastic sphere of radius R is approaching an infinite rigid plate with a velocity under a constant load. The lubricant in the system is taken to be a compressible fluid. Under the usual assumption of EHL applicable to a thin film, the reduced momentum equations and the continuity equation governing the motion of the lubricant in polar coordinates can be obtained. Integrating the reduced momentum equations with the no-slip-boundary conditions, the velocity components are then obtained. Substituting velocity components into continuity equation and integrating across the film thickness with the boundary conditions of *v(r,z) i.e. v(r,h)=∂h/∂t,* we can then derive the transient Reynolds equation in polar coordinates as:

$$\frac{\partial}{\partial r}\left(\frac{\rho r h^3}{\mu} f(l,h)\frac{\partial p}{\partial r}\right) = 12r\frac{\partial}{\partial t}(\rho h) \tag{3}$$

where

$$f(l,h) = 1 - 12\left(\frac{l}{h}\right)^2 + 24\left(\frac{l}{h}\right)^3 \tanh\left(\frac{h}{2l}\right) \tag{4}$$

or in dimensionless form as:

$$\frac{\partial}{\partial X}\left(\varepsilon XF\frac{\partial P}{\partial X}\right) = KX\frac{\partial}{\partial T}(\bar{\rho}H) \tag{5}$$

where $\varepsilon = \bar{\rho}H^3/\bar{\mu}$, $K = 8\pi/W$

$$F(L,H) = 1 - 12\left(\frac{L}{H}\right)^2 + 24\left(\frac{L}{H}\right)^3 \tanh\left(\frac{H}{2L}\right) \tag{6}$$

The radial coordinate, X, is with its origin in the center of the contact. The boundary conditions for Eq. (5) are:

$$P(X \to \infty, T) = 0 \tag{7a}$$

$$\partial P(0,T)/\partial X = 0 \tag{7b}$$

$$P(R,T) \geq 0 \tag{7c}$$

2.2 Rheology equations

As the pressure increases with time, the elastic deformation and the effect of pressure on the viscosity and density cannot be neglected. This stage is denoted as the high-pressure stage. The pressure dependence of viscosity and density is an important issue of the present problems.

The viscosity of the lubricant is assumed to be the function of pressure only. The relationship between viscosity and pressure used by Roelands [13] can be expressed as:

$$\bar{\mu} = \exp\{(9.67 + \ln\eta_0)[-1 + (1 + 5.1\times10^{-9}p)^{z'}]\} \tag{8}$$

where η_0 is the viscosity under ambient pressure, and z' is the pressure-viscosity index. According to Dowson and Higginson [14], the relationship between density and pressure is given as:

$$\bar{\rho} = \frac{\rho}{\rho_0} = 1 + \frac{0.6\times10^{-9}p}{1 + 1.7\times10^{-9}p} \tag{9}$$

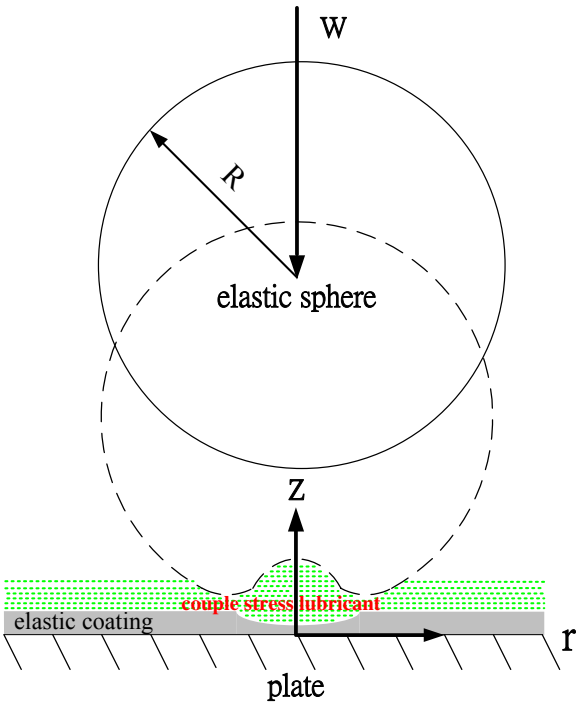

Fig. 1. Geometry of EHL under pure squeeze motion.

2.3 Elasticity equation

The film thickness within the EH conjunction can be written as:

$$h(r,t) = h_0(t) + r^2/2R + \delta(r,t) + \zeta(r,t) \tag{10}$$

To calculate the static deformation of elastic sphere caused by pressure distribution, influence coefficients D_{ij} are introduced. The deformation can thus be computed at discrete points i as a sum of the deformation contributions from all pressure points j :

$$\delta_i = \sum_{j=1}^{n} D_{ij}P_j \tag{11}$$

Within the frame of linear elasticity, the normal deformation of coating is given by [8]

$$\zeta(r,t)=\frac{2\alpha}{d}\int_0^a \int_0^\infty [L(\omega)J_0(\frac{r\omega}{d})J_0(\frac{s\omega}{d})d\omega]p(s)sds \quad (12)$$

Where

$L(\omega)=(2\kappa\sinh 2\omega-4\omega)/(2\kappa\cosh 2\omega+4\omega^2+k^2+1)$,

$\alpha=(1-\nu^2)/E$, and $\kappa=3-4\nu$. J_0 is the Bessel function of the first kind of order zero and ν is Poisson's ratio.

The dimensionless film thickness between two elastic bodies with coating in circular contacts can be expressed as:

$$H_i=H_0+\frac{X_i^2}{2}+\sum_{j=1}^{n}D_{ij}P_j+\bar{\zeta}_i \quad (13)$$

where the influence coefficients, D_{ij} , are computed according to Yang and Wen [1] and Larsson and Höglund [4].

2.4 Load balance equation

The instantaneous load balance equation for a constant load condition is:

$$\int_0^\infty PXdX=1/3 \quad (14)$$

3 Numerical solution

The finite difference method (FDM), Gaussian elimination, and the Gauss-Seidel iteration method are used to solve the transient modified Reynolds equation with its boundary condition, the elasticity deformation equations of ball and coating layer, load balance equation, and lubricant rheology equations simultaneously. Equation (5) has to be discretized and solved at a finite number of locations along the radial coordinate axis X. The discretized form of the Equation (5) can be derived as:

$$(A_i+B_i)P_{i+1}-2B_iP_i+(B_i-A_i)P_{i-1}=$$
$$KX_i(\bar{\rho}\frac{H-H^{k-1}}{\Delta T}+H\frac{\bar{\rho}-\bar{\rho}^{k-1}}{\Delta T})_i \quad (15)$$

where

$A_i=(X\,\partial\varepsilon F/\partial X+\varepsilon F)_i/(2\Delta X)$, $B_i=(X\varepsilon F/\Delta X^2)_i$, ΔX is the mesh size, i. e., $\Delta X=X_i-X_{i-1}$, the superscript k, denoting discretization in time, ΔT is the time increment, i. e., $\Delta T=T^k-T^{k-1}$. The boundary condition (7b) at X=0 can be derived by fitting a second degree polynomial as:

$$3P_1-4P_2+P_3=0.0 \quad (16)$$

Apply boundary condition (7c) to the first three grid points at X=0. For the constant load case, the rigid separation is an unknown variable in each time step. It can be determined by solving the transient Reynolds equation with the load balance equation.

4 Results and Discussions

To discuss the effects of flow rheology and elastic deformation (δ) of spheres and coating (ζ) on the squeezing motion, the point contact EHL problems are discussed under the conditions of non-isoviscous, compressible lubricant, and constant load. Numerical solutions of film profiles (*h*) and pressure distributions (*p*) in pure squeeze motion are calculated using the parameters listed in Table 1. The initial falling height of the sphere is $20\mu m$. A typical problem with coating thickness, $\zeta=2a$, $W=5.24\times10^{-9}$, $G=3500$, E_b =220 GPa, $\nu_b=0.3$, and $\nu_c=0.3$ is solved.

Table 1. Computational data.

Inlet viscosity of lubricant, Pa-s	0.04
Inlet density of lubricant, kg/m^3	846
Pressure viscosity coefficient (α), 1/GPa	15.91
Pressure-viscosity index (Roelands)	0.4836
Equivalent radius of elastic ball, m	0.02
Elastic modulus of coating, GPa	110~330
Elastic modulus of balls, GPa	220
Poisson's ratio of ball	0.3
Poisson's ratio of coating	0.3
Density of balls, kg/m^3	7850

The upper limit of the computational region in the beginning is chosen as X_{max}=16.0. The Reynolds equation is discretized by the central difference technique in the space domain and the explicit technique in the time domain. When more than half of the region was cavitated, the maximum analyzed region X_{max} reduces to half of its initial region, and so on, until X_{max}=2.0. The grid was made up of 401 nodes, which are evenly distributed, in every calculating domain. The Gauss-Seidel iteration method is employed to calculate the film thickness and pressure distribution at each time step.

In the case of constant load conditions, Figure 2 shows the relative change in the *p* and *h* for a flexible sphere approaching a lubricated coating surface with couple stress lubricant. It is observed from Figure 2 that the *p* is quite flat at relatively large *h*, but it becomes steeper with decreasing *h*. It was found that the p_c gradually increases with decreasing h_c from 2.6ms to 15.7ms when the h_c decreases to 33nm. As time goes on, the *h* will decrease, and the contact region will reach the Hertz contact condition.

The *p* of couple stress lubricant is greater than that of Newtonian lubricant at central region. As the loading is constant, the integration of the pressure distribution over the loading area is a constant. Therefore, the *p* found reverse at outside central region. As seen in Figure 2, the *h* decreases gradually as the squeeze proceeds. The *h*

of couple stress lubricant is greater than that of Newtonian.

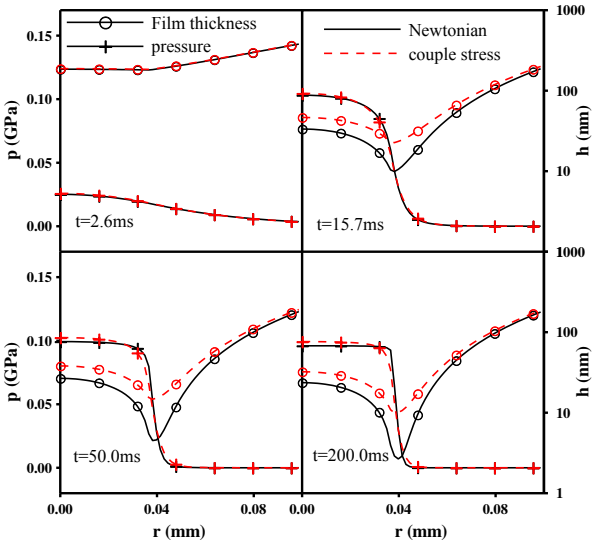

Fig. 2. p and h distribution versus time using different models

Figure 3 shows the central pressure and film thickness versus time under constant load condition. The p_c increases rapidly with time at the initial stage. Meanwhile, the p_c increases quickly to a maximum. Then the p_c decreases slowly to near the amplitude of the well-known Hertzian pressure with time at the final stage. This stage can be considered as the quasi-static condition. This stage keeps longer time. The h_c decreases rapidly with time at the initial stage. Then, they decrease slowly with time. The p_c with coating is smaller than that without coating. The h_c with coating is greater than that without coating. The h_{min} with coating is greater than that without coating at the initial stage. The h_{min} with coating is smaller than that without coating from 14ms to 60ms. The h_{min} with coating is greater than that without coating at the final stage.

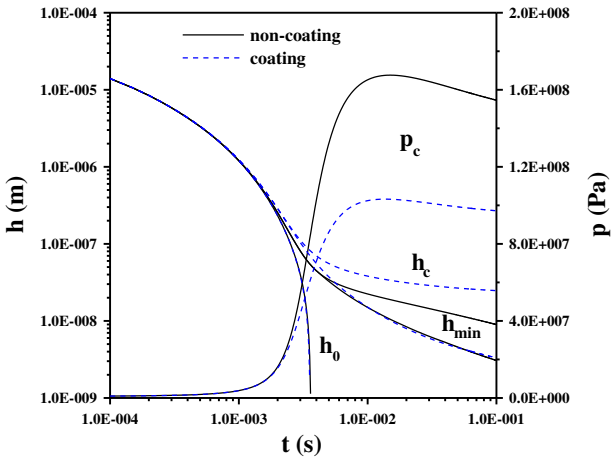

Fig. 3. p_c and h versus time with/without coating.

Figure 4 shows the central pressure and film thickness versus time under constant load condition for different E and ζ. It is observed from Figure 4 that the greater the E, the greater the p_c, and the smaller the h_c. The greater the ζ, the smaller the p_c, and the greater the h_c.

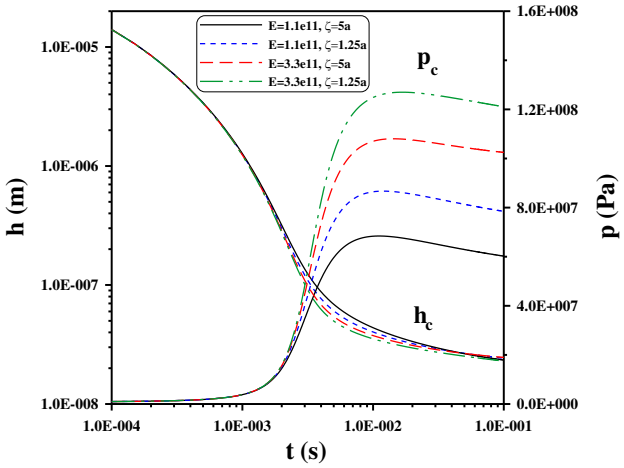

Fig. 4. p_c and h_c versus time with various E and ζ.

Figure 5 shows the p and h for different E in r-direction under constant load condition at t=0.1s. At central region, the greater the E, the greater the p, and the smaller the h. The film thicknesses and pressures are is found reverse at outside central region. The smaller the E, the greater the positions of minimum film thickness.

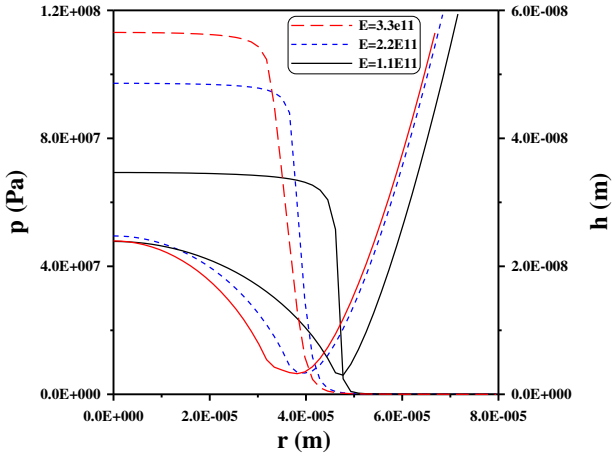

Fig. 5. p and h versus radius with various E.

Figure 6 shows the p and h for different ζ in r-direction under constant load condition at t=0.1s. At central region, the greater the ζ, the smaller the p, and the greater the h. The film thicknesses and pressures are found reverse at outside central region. The greater the ζ, the greater the positions of minimum film thickness.

Figure 7 shows the relationship of the central normal squeeze velocity (v_c) and the h_c using present models under constant load condition. The v_c decreased rapidly with decreasing h_c at the initial stage. The greater the E, the greater the v_c. The greater the ζ, the smaller the v_c.

Figure 8 shows the central pressure and film thickness versus time under constant load condition for different l. It is observed from Figure 8 that the greater the l, the greater the p_c, and the greater the h_c and h_{min}.

The time needed to achieve maximum p_c increases with increasing l. Similarly, the time needed to achieve the Hertzian pressure also increases with increasing l.

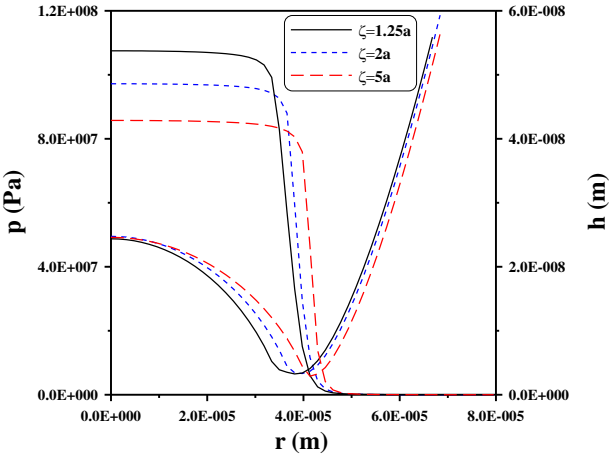

Fig. 6. p and h versus radius with various ζ.

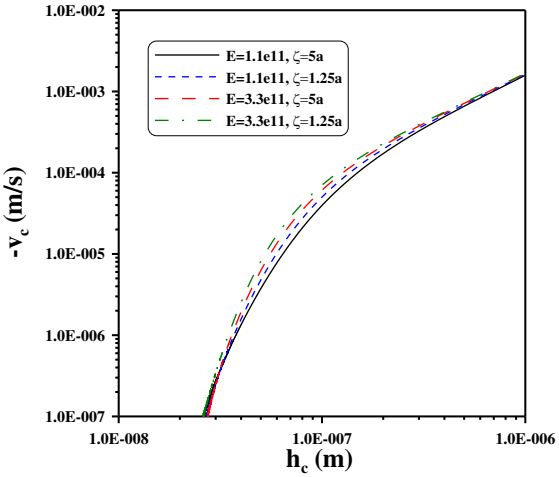

Fig. 7. Variation of v_c versus h_c various E and ζ.

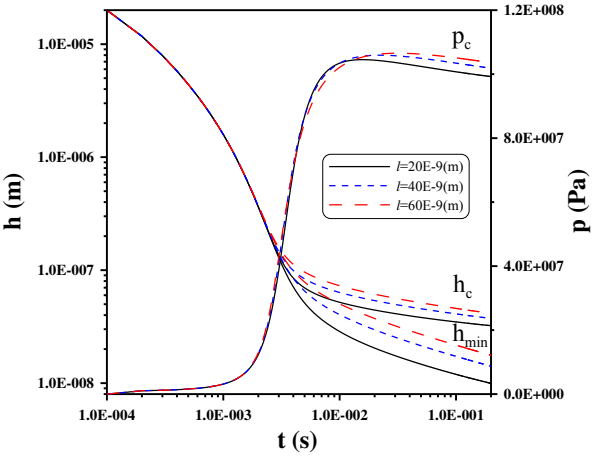

Fig. 8. p_c and h versus time with various l.

Figure 9 shows the p and h for different l in r-direction under constant load condition at t=0.1s. At central region, the greater the l, the greater the p, and the greater the h. The pressures are found reverse at outside central region.

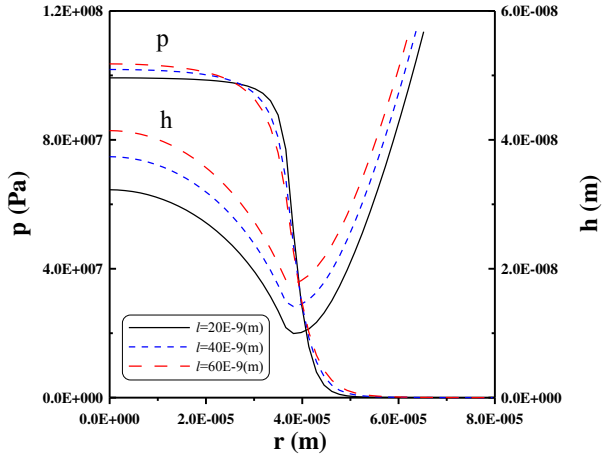

Fig. 9. p and h versus radius with various l.

5 Conclusions

In this study, a numerical method for general applications was developed to investigate the effects of the isotropic coating at pure squeeze EHL motion of circular contacts under constant load conditions using FDM. The conclusions from the main results can be summarized as follows:

1. At central region, the greater the E, the greater the p, and the smaller the h. The h and p is found reverse at outside central region.
2. At central region, the greater the ζ, the smaller the p, and the greater the h. The h and p is found reverse at outside central region.
3. The greater the l, the greater the h. At central region, the greater the l, the greater the p, the p is found reverse at outside central region.
4. The positions of minimum film thickness for smaller elastic modulus are greater than that for larger elastic modulus. The positions of minimum film thickness for greater coating thickness are greater than that for smaller coating thickness.
5. The greater the E, the greater the v_c. The greater the ζ, the smaller the v_c.

Acknowledgments

The authors would like to express their appreciation to the Ministry of Science and Technology (MOST 105-2221-E-143 -005) in Taiwan for financial support.

References

1. P. R. Yang, and S. Z. Wen, *Wear*, **142**(1), 17 (1991)
2. L. Chang, *ASME J. Applied Mech.*, **63**(2),347 (1996)
3. D. Dowson and D. Wang, *Wear*, **179**(1-2),29 (1994)
4. R. Larsson and E. Högund, *ASME J. Tribol.*, **117**(1), 94 (1995)

5. M. M. A. Safa and R. Gohar, *ASME J. Tribol.*, **108**(1), 372 (1986)
6. A. Elsharkawy and B. Hamrock, *Proc. Inst. Mech. Eng. Part J. J. Eng. Tribol.*, **209**(2), 119 (1995)
7. K. L. Johnson, Contact Mechanics, Cambridge university press, Cambridge, UK, (1987)
8. M. J. Jaffar, Proc. *Inst. Mech. Eng. Part J. J. Eng. Tribol.*, **222** (1), 61 (2008)
9. Y. Liu, W. W. Chen, D. Zhu, S. Liu, and Q. J. Wang, *J. Tribol.-Trans. ASME*, **129**(3), 509 (2007)
10. W. Habchi, *Tribology International*, **73**, 57 (2014)
11. L. M. Chu, C. C. Yu, Q. D. Chen, W. L. Li, *Journal of Tribology*, ASME, **137** (1), 011503-1 (2015)
12. V. K. Stokes, Couple stresses in fluids, Phys. Fluids, **9**, 1709 (1966)
13. D. Dowson and G. R. Higginson, Elastohydrodynamic Lubrication, Pergamon, Oxford, UK, 88 (1966)
14. C. J. A. Roelands, J. C. Vlugter, and H. I. Watermann, *ASME J. Basic Eng.*, **85**(4), 601 (1963)